Niessink Tom (Orcid ID: 0000-0002-8621-9868)

The diagnostic accuracy of Raman spectroscopy integrated with polarized light microscopy for calcium pyrophosphate associated arthritis

Tom Niessink, MSc. [1,2*], Matthijs Janssen MD., PhD[2], Tanja Giesen, MSc.[2], Monique N. Efdé, MD.[2], Antoaneta C. Comarniceanu, MD.[2], Cees Otto, PhD.[1], Tim L. Jansen MD., PhD[2]

[1] University of Twente, Enschede, the Netherlands

[2] VieCuri Medical Centre, Venlo, the Netherlands

TN: ORCiD: 0000-0002-8621-9868,

TG: ORCiD: 0000-0002-1632-4232

MNE: ORCiD: 0000-0002-0854-4374,

ACC:

MJ: ORCiD: 0000-0003-3700-6257,

CO: ORCiD: 0000-0001-6955-4843,

TLJ: ORCiD: 0000-0003-3026-3154,

* Corresponding author: t.niessink@utwente.nl, Personalized Diagnostics and Therapeutics, University of Twente, Drienerlolaan 5, 7500AE Enschede, The Netherlands.

Acknowledgements

None to be reported.

Funding

The collaboration project is co-funded by the PPP Allowance made available by Health-Holland, Top Sector Life Sciences & Health, to Stichting ReumaNederland to stimulate public-private partnerships.

VieCuri Medical Centre, Venlo, the Netherlands, partially funded the production and use of the H-iRPolM Raman Spectroscope.

This article has been accepted for publication and undergone full peer review but has not been through the copyediting, typesetting, pagination and proofreading process which may lead to differences between this version and the Version of Record. Please cite this article as doi: 10.1002/acr.25350

Abstract

Background

We studied the performance of integrated Raman Polarized light Microscopy (iRPolM) for the identification of calcium pyrophosphate (CPP) associated arthritis (CPPD)

Methods

This is a diagnostic accuracy study including 400 consecutive synovial fluid samples from a single hospital in the Netherlands. Accuracy measures were calculated against polarized light microscopy (PLM) and the 2023 ACR/EULAR criteria set for CPPD.

Results

The interrater reliability between iRPolM and the 2023 ACR/EULAR criteria set for CPPD was strong (k = 0.88). The diagnostic performance of iRPolM compared to the 2023 ACR/EULAR criteria set was: sensitivity 86.0% (95%CI 73.3–94.2), specificity 99.1% (95%CI 97.5–99.8), positive likelihood ratio 100.33 (95%CI 32.3–311.3), negative likelihood ratio 0.14 (95%CI 0.07–0.28), positive predictive value 93.5% (95%CI 82.2–97.8), negative predictive value 98.0% (95%CI 82.2–97.8), and accuracy 97.5% (95%CI 95.5–98.8). We allowed rheumatologists to rate the certainty of their microscopic identification of CPP and found a large correspondence between iRPolM and a certain identification (κ = 0.87), while only 10% of the uncertain CPP identifications could be confirmed with iRPolM. We identified several novel particle types in synovial fluid analysis, including calcium carbonate crystals, deposited carotenoids, microplastics, and three types of Maltese cross birefringent objects.

Conclusion

iRPolM can easily identify CPP crystals with a strong diagnostic performance. PLM alone is not specific enough to reliably resolve complicated cases and the implementation of Raman spectroscopy in rheumatology practice can be of benefit to patients with suspected CPPD.

242 words

Keywords: calcium pyrophosphate, diagnostic accuracy study, Raman spectroscopy, Maltese crosses, microplastics

Significance and innovation

- In this study it is demonstrated how Raman spectroscopic analysis of synovial fluid can be used as a highly specific (99.1%) and highly sensitive (86.0%) method to identify CPP in a large cohort of unselected patients.

- Due to the chemical specific nature of the modality, we were not only able to identify CPP, but also to characterize a large number of objects in synovial fluid analysis, including novel particle types such as calcite crystals, carotenoid deposits, Maltese crosses, and microplastics.

- Raman spectroscopy can be implemented in rheumatology practice as a reliable diagnostic method for CPP associated arthritis. Furthermore, the ability to identify previously unknown particles in synovial fluid will allow for increased patient stratification and potentially open new therapeutic pathways in rheumatology.

Introduction

Crystal associated arthropathies, predominantly gout and calcium pyrophosphate associated arthritis (CPPD), are the most common forms of inflammatory arthritides worldwide[1]. According to ACR/EULAR classification criteria sets, the identification of monosodium urate (MSU) or calcium pyrophosphate (CPP) crystals in synovial fluid leads to a definitive classification of gout and CPPD[2,3]. In clinical practice, crystals are commonly identified with polarized light microscopy (PLM). This method is known to be flawed in CPPD however, due to poor interrater reliability, lack of training, subjectivity (confirmation bias), and sensitivity to artefacts[4-8]. Furthermore, CPP crystals are low in birefringence and therefore sometimes difficult to localize with polarized light microscopy. The application of Raman spectroscopy can potentially overcome these shortcomings with increased specificity, as Raman spectra are unique chemical fingerprints of the analyte. A first proof-of-principle was already published in 1991 by McGill et al[9]. Recent Raman spectroscopic technology for the identification of crystals include a transdermal in-vivo Raman probe[10], a point-of-care Raman spectroscope[11], stimulated Raman spectroscopy[12], hyperspectral Raman imaging[13], and laser-confocal micro-Raman spectrometry[14].

MSU and CPP are not the only known synovial fluid crystals, and several other types are known to be confounders in joint disease[13,15,16]. Basic calcium phosphate crystals, predominately calcium hydroxyapatite, are pro-inflammatory and are frequently found in osteoarthritis[17]. These crystals lack birefringent properties and are therefore not identifiable with PLM. Calcium oxalate crystals are birefringent but rarely identified and potentially even misclassified[4,18]. Lipid conglomerates such as Maltese cross birefringent spherules and cholesterol monohydrate plates can be identified by skilled

microscopist, although their clinical significance is ambiguous[19]. Furthermore, frequently used intra-articular injected drugs such as glucocorticoids can be present long after administration as amorphous birefringent objects, which can act as a strong confounding factor in diagnosing CPPD. Raman spectroscopy can provide chemical specific identifications for all these confounders[13].

We have previously demonstrated the diagnostic performance of a combined approach for acute gouty arthritis[20]. We integrated a Raman spectroscope in a polarized light microscope (iRPolM) and tested this on a cohort of 200 consecutive patient samples. In this cohort, we reached a sensitivity of 77.6% (95% CI 65.8-86.9) and specificity of 97.7% (95% CI 93.5-99.5) when we defined gout based on the 2015 ACR/EULAR gout classification criteria. We saw a strong correspondence between iRPolM and polarized light microscopy, with a Cohen's κ of 0.90 (near perfect interrater agreement). Recently, a joint group of crystal dedicated researchers published the 2023 ACR/EULAR CPPD classification criteria[2]. Here we have applied these novel criteria to investigate the diagnostic performance of iRPolM for CPPD in a cohort of 400 consecutive patient samples.

Method

Study design and participants

This study is a prospective single-hospital diagnostic accuracy study. We collected a consecutive series of synovial fluid samples from patients visiting the outpatient rheumatology clinic of VieCuri Medical Centre (Venlo, the Netherlands) between 1 April 2022 and 1 November 2023. We collected all available samples and did not preselect on clinical diagnosis, a priori likelihood of CPPD, or else. Eligible for inclusion were all patients above 18 years of age who underwent a joint puncture in any swollen

peripheral joint as part of their routine diagnostic and clinical care. Only clinical waste synovial fluid was used in this study. Clinical data was retrieved from the patient's electronic health records.

The sample size of 400 patients was determined to be sufficient using the formula for sample size estimation in diagnostic accuracy studies[21]. The prevalence of CPPD when identified with Raman spectroscopy in a similar cohort of unselected synovial fluid samples was 13%[11]. We set the maximum width of the 95% confidence interval to 10% and the significance to 0.05.

Patients gave written informed consent for use of their synovial fluid waste material and data. This study was conducted according to good clinical practice and the adapted Helsinki declaration. The ethics committee of Maastricht University Medical Centre gave an exemption for ethics board review (METC AzM/UM, 2022-3098-A-3). The board of directors of VieCuri Medical Centre reviewed and approved the study protocol. This study is reported and conducted according to the Standards for Reporting Diagnostic accuracy studies (STARD) guidelines[22]. The funders of the study had no role in study design, data collection, data analysis, data interpretation, or writing of the manuscript.

Test methods

From each fluid sample a 40μl droplet was placed on a microscope slide (Epredia, Michigan, USA) and covered with a coverslip (Menzel-Gläser, Germany). The slides were analysed by a single trained rheumatologist (MNE, ACC, TLJ, all >10 years of experience) for the presence of MSU and/or CPP crystals with a Zeiss Axiolab 5 polarized light microscope (CarlZeiss AG, Jena, Germany). The rheumatologist

performing the analysis was the treating specialist for that patient and was therefore not blinded for the clinical presentation. The sample was scored positive for CPP when one or more positive birefringent tubular-shaped or rhomboid-shaped crystals were identified. If for any reason, such as artefacts or low crystal count, the identification could not be given with 100% certainty by the rheumatologist, the sample was scored as uncertain for CPP.

Patients were classified as CPPD when they scored positive on the 2023 ACR/EULAR CPPD classification criteria set[2]. All included patients were subjected to the classification scheme analysis. According to the 2023 ACR/EULAR CPPD classification criteria set, a certain identification of crystals with PLM or radiographic proof of crowned dens syndrome leads to a definitive CPPD classification. If crystal proof cannot be given, patients are scored on the presentation and course of the disease and imaging. The CPPD classification score ranges from -11 to 83 points and patients are classified as positive for CPPD if more than 56 points are scored. This threshold was tested to have a specificity of 87.9% and sensitivity of 97.8% within a cohort of 226 patients[2]. When the outcome of PLM was considered indefinite (for example due to artefacts, uncertain crystal identification), no points are scored or subtracted for this criterion. When data were unavailable, no points were awarded on that specific domain as described in the 2023 ACR/EULAR CPPD classification criteria set. We calculated the CPPD classification score for all patients included in the study.

The samples were then analysed with the iRPolM Raman spectroscope (Hybriscan Technologies B.V.), independently from the analysis by the rheumatologists. The iRPoLM measurements were performed as soon as possible after fluid draw, with a

maximum of three days. Samples were stored at room temperature within the syringe and were not centrifuged before analysis. With this device, birefringent objects are localized with a standard polarized light microscope by a trained analyst (TN), who manually selects objects of interest which are then scanned with the integrated Raman spectroscope. The device operates a 532 nm green light laser, with a 10mW under-the-objective laser power. For each object, the Raman spectrum was measured between 0-3600 cm^{-1} with an integration time of 1 second per pixel. Depending on crystal size, 60-120 pixels were measured, with a total measurement time between 1 and 2 minutes. Up to 10-20 different objects could be measured per patient. The measured spectra were compared to earlier reported spectra of CPP[9,11]. A patient was considered positive for CPP if one or more crystals of that type could be identified with Raman spectroscopy. As iRPolM is not yet certified for clinical diagnostics, the results were considered research use only and not reported back to the rheumatologists.

Analysis

Diagnostic accuracy measures, with corresponding 95% confidence intervals, were calculated using 2x2 contingency tables. We calculated accuracy measures in four scenarios. In the first scenario, iRPolM against the 2023 ACR/EULAR CPPD criteria set (which includes PLM), we regarded uncertain PLM outcomes as not performed (no subtraction of points). In the second scenario, iRPolM against the 2023 ACR/EULAR CPPD criteria set (which includes PLM), we regarded uncertain PLM outcomes as negative (thus subtraction of -1 point or -7 if two or more fluids were negative for CPP). In the third scenario, we regarded all PLM CPP crystal identifications (certain and uncertain) as a positive test outcome, and we then compared iRPolM against PLM as the reference test. In the fourth scenario, we regarded only the certain PLM CPP

crystal identifications as a positive test outcome, and all uncertain PLM CPP identifications were regarded negative. In all scenario's, all 400 samples were included in the analysis. For every scenario, we calculated the sensitivity, specificity, positive likelihood ratio, negative likelihood ratio, positive predictive value, negative predictive value, and accuracy. The correspondence between the reference tests and iRPoIM in the identification of CPP was estimated with Cohen's Kappa (κ) interrater reliability test. A $\kappa < 0.20$ indicates no agreement, $0.21 < \kappa < 0.39$ indicates a minimal agreement, $0.40 < \kappa < 0.59$ indicates a weak agreement, $0.60 < \kappa < 0.79$ indicates a moderate agreement, $0.80 < \kappa < 0.89$ indicates a strong agreement and $\kappa > 0.90$ indicates a near perfect agreement[23]. All calculations were performed with MATLAB R2023a (MathWorks corporation, Massachusetts, USA).

Results

A total of 410 samples were delivered for analysis with iRPoIM. Ten samples were excluded: one because of the patient's age being below 18 years, and nine samples were too dehydrated to perform a reliable analysis. A total of 400 samples were included, samples were analysed with iRPoIM within three days (mean 1.1 day ± 1.6 SD) after synovial fluid draw. Using PLM, 40 patients had a direct proof of CPPD because of certain CPP crystal identification. An additional 10 patients were classified as CPPD by the 2023 ACR/EULAR CPPD criteria set[2]. In these 10 patients the outcome of synovial fluid analysis by rheumatologists using PLM was scored uncertain but suspicious for CPP. The total number of patients classified with CPPD according to the 2023 ACR/EULAR CPPD criteria set was 50. No patients were classified as CPPD via radiographic presence of crowned dens syndrome.

The mean age of all patients was 66.2 years (SD ±15.2), CPPD patients were 74.8 (SD ±10.2) years old on average. The complete cohort included 257 males (64.3%), and 60.0% of the CPPD patients were male. We collected no precise data on race or ethnicity, but the patients were predominantly white Europeans. CPPD was mostly classified in patients with swollen knee joints (76.0%) or wrists (12.0%). Alternative diagnoses included gout (39.7% according to 2015 ACR/EULAR gout classification criteria[3]), rheumatoid arthritis (11.4%), osteoarthritis (10.0%), bacterial joint infections (3.2%), and for 35.7% of the patients no definitive alternative diagnosis was available. The flow of participants and a full overview of patient characteristics is given in **figure 1**, **table 1**.

In the first scenario we compared iRPolM with the 2023 ACR/EULAR CPPD classification criteria set, and we considered all uncertain identifications as not performed (no points subtracted). In this scenario, iRPolM identified CPP crystals in 46 samples. There was a correspondence between iRPolM identification and the 2023 ACR/EULAR CPPD classification criteria set in 43 patients. Of these 43, 38 were classified directly via a certain identification of CPP in synovial fluid by PLM, and an additional 2 patients were classified as CPPD by having >56 points according to the criteria set. Another 3 patients were positive for CPP using iRPolM but were negative according to the 2023 ACR/EULAR CPPD classification criteria set. Two of these patients were clinically diagnosed with rheumatoid arthritis and one with an unspecified seronegative arthritis. If iRPolM would be applied as a definite proof of CPPD, it would lead to a 7% increase in CPPD diagnoses with respect to the 2023 ACR/EULAR CPPD classification criteria set. A full overview of all diagnostic characteristics is given in **table 2**. We saw no significant differences in terms of performance measures between analysed joint types nor between sex groups.

In the second scenario we also compare iRPolM with the 2023 ACR/EULAR CPPD classification criteria set, but we now considered uncertain CPP classifications with PLM as negative. This leads to subtraction of 1 (one time negative) or 7 (two or more times negative) points on the total CPPD score. For a total of 7 patients, the score changes. 3 iRPolM negative patients which were classified as CPPD in scenario 1 are now classified negative, which slightly increases the sensitivity of iRPolM with respect to the first scenario. However, in this scenario the number of patients whose diagnosis was missed with the criteria set but was confirmed with iRPolM now increases from 3 to 7.

In scenario three we compared iRPolM with PLM, and we scored all uncertain CPP identifications as positive. In this worst-case scenario, iRPolM demonstrated a sensitivity of 51.2%. In scenario four we again compared iRPolM with PLM but scored all uncertain CPP identifications as negative. In this best-case scenario, iRPoLM demonstrated a sensitivity of 95%. Clearly, a high number of cases had uncertainty in the identification of CPP crystals with PLM by the trained rheumatologists. Of 88 samples with CPP crystal identifications, a certain identification was given in 40. Almost all certain crystal identifications with PLM were indeed confirmed as CPP by iRPoLM (95% agreement). Only 7 of the 48 uncertain PLM CPP identifications were additionally identified as CPP with iRPolM. An additional 5 patients with uncertain crystal identifications could be classified as CPPD with the 2023 ACR/EULAR CPPD classification criteria set. Several novel particles were identified during this study: some of these (calcite, carotenoids, microplastics, glucocorticoid crystals) are potential mimickers for CPP in their presentation in the synovial fluid, which were

frequently identified in the samples with an uncertain identification of CPP (**figure 2, supplementary table 1, supplementary figure 1**).

In 20% of uncertain CPP crystal identifications, iRPolM identified the positive birefringent particles present in the synovial fluid samples as calcite crystals (calcium carbonate[15]). A full overview of iRPoLM identifications of all uncertain CPP crystal identifications is given in **supplementary table 1**. Cholesterol monohydrate presents as large plate-like deposits with notched corners and a distinctive Raman spectrum and were identified in 2 out of 400 patients. A novel organic deposition we discovered are Carotenoid birefringent objects, presenting as fluffy, positive birefringent rhomboids with similarities to CPP. These particles are known to form benign deposits in the stratum corneum[24] but, to our knowledge, have not been reported before in synovial fluid samples. Furthermore, we identified BCP crystals in 8 patients (2%), 2 of these were clinically diagnosed with RA, 1 with gout, 4 with unspecified arthritis, and one with erosive hand OA.

Microplastics (MP) were highly prevalent in the analysed synovial fluid samples. In a total of 73 samples, MPs were identified, in 4 distinct types: polyethylene (PE), polystyrene (PS), polypropylene (PP), and polyethylene terephthalate (PET). 67 samples contained one type of MP, and 6 samples had two distinct types of MPs. 7 patients with MPs had an orthopaedic implant in the index joint, 8 patients had an orthopaedic implant at a distant joint. All synovial fluid samples were drawn in a standard rheumatology practice, using (polypropylene) BD Plastipak® syringes and samples were prepared using ordinary microscope slides. This environment and protocol are not fit for the high standards required for microplastic research and, while

these results are interesting, these are inconclusive for the presence of MPs in synovial fluids.

With iRPolM, we identified three different types of Maltese cross birefringent objects, each with distinct Raman spectra (**figure 3**). Two patients had Maltese cross-like monosodium urate deposits, which manifested as a dehydration artefact in synovial fluid when the samples were re-examined the day after initial analysis. Both patients were hyperuricemic, only one patient was clinically diagnosed with gout (crystal proven). Another two patients had Maltese cross birefringent spherules with a spectrum distinct for polysaccharides, such as glycogen or starch[25], with distinct peaks at 477, 866, 937, 1002, 1337, 1457, 2907 cm^{-1}. There was one patient with Maltese cross birefringent spherules demonstrating a lipid-like spectrum, which closely matched earlier described, including specific bands for cholesterol (at 702, 1442, and 1669 cm^{-1})[13].

There are no adverse events to be reported.

Discussion

The main conclusion of this study is that integrated Raman spectroscopy with Polarized light microscopy (iRPolM) is a more objective and highly specific method to identify crystals in CPPD patients compared to PLM. One of the primary advantages of iRPolM is the chemical specificity. Three cases were present in which iRPolM identified CPP crystals which were missed with PLM and/or the criteria sets. The analysis of synovial fluid samples takes 5-15 minutes per patient and a single Raman spectroscope can therefore have a high throughput.

Although CPP crystal identification with PLM is reported to have low sensitivity[4], we here demonstrate that especially uncertainty plagues clinicians during their PLM analyses. Only 14.6% of uncertain CPP identifications with PLM could be confirmed with Raman spectroscopy. We identified several novel particles which can mimic the presentation of CPP. Cholesterol monohydrate plates, Maltese crosses, and deposited glucocorticoids are rarely identified in synovial fluid[26,27]. These organic objects have no apparent role in inflammation but are mostly associated with non-crystal related joint disease[19,28,29]. Earlier reports describe Maltese crosses as either 'calcium carbonates along with a proteinaceous organic phase'[30], or as lipid spherules[19]. We here demonstrate that several compounds can present as Maltese crosses and the presentation is not specific. Polysaccharides, one of the novel designations of Maltese crosses, are an important component of synovial fluid, mostly in the form of hyaluronic acid[31]. The measured spectra, however, most closely resemble glycogen[32], which is an important form of molecular energy storage in humans. Charcot-Leyden crystals are earlier reported in synovial fluid[4,33] but not identified in our cohort. Some of the novel found objects, however, are frequently present in synovial fluid and not easily identified with polarized light microscopy. BCP crystals are commonly associated with OA and are highly present in advanced disease[34]. The relatively low prevalence of BCP is interesting and might partially be attributed to the fact that patients with advanced OA in the Netherlands are most often referred to orthopaedic clinics and therefore could only sparsely be included in this study.

As our research setting was not optimized for microplastic research we remain to be inconclusive on the whereabouts of microplastic material in the samples. Microplastics have already been identified in ex vivo blood samples from healthy donors[35] and

recently have been identified in synovial tissue[36]. Raman spectroscopy can be used for further studies to a potential role between arthritis and microplastics. Calcite crystals are reported before and their common presence in synovial fluid makes them an interesting research item, potentially as a biomarker for osteoarthritis[37]. Furthermore, Raman spectroscopic analysis enables not only the differentiation between crystal types, but also differentiation between crystal structures of the same type. There are four theorized types of CPP (triclinic CPP, monoclinic CPP, amorphous CPP, and monoclinic CPP tetrahydrate beta)[38], and we identified one. In vitro studies have demonstrated a difference in inflammatory potential between these crystal types. The ability to differentiate between CPP crystal structures could therefore be relevant for advanced CPPD phenotyping and disease prognosis.

Strong points of this study are the large cohort of non-selected fluid samples and the comparison of iRPolM with both the results of PLM and clinical data. Furthermore, the outcome of the Raman spectroscopic analysis was blinded for the rheumatologist operating the polarized light microscope. This study also had limitations. As is customary in clinical practice, the presentation of disease was known to the analyst performing PLM. This could lead to a conformation bias of PLM and an artificial increase of the sensitivity of PLM with respect to iRPolM. Rheumatologists from one hospital with a special dedication to PLM reviewed the samples and the outcomes might not represent how clinicians from other centres would have performed on average. CPP identification in both iRPolM and particularly PLM rely on operator skill and opinion and are therefore not perfectly objective. Additionally, as we used only a single observer for PLM, our results might be impacted by the poor interrater reliability

for PLM. In iRPolM, localization of CPP crystals is still a manual operation and rare particles therefore might be missed.

Identification of CPP crystals in synovial fluid is a direct proof of the disease. We here demonstrated that the current standard, polarized light microscopy, is lacking the required specificity to make 100% reliable decisions regarding CPP arthritis therapy and treatment plans. Raman spectroscopic identification of CPP, however, is undisputable and therefore is an addition to routine synovial fluid analysis. With these results and earlier positive results for gout, iRPoLM has demonstrated a strong feasibility for clinical use[20]. In our future efforts we will proceed to work towards a clinically certified specific method for crystal identification.

Data sharing

Scores on individual elements of the 2023 ACR/EULAR CPPD classification criteria and the outcome of Raman analysis for individual patients are available on the 4TU.Researchdata repository: https://data.4tu.nl/portal. The full study protocol is available on our institute website www.utwente.nl.

Author contributions

TN: conceptualisation, data curation, formal analysis, software, investigation, visualisation, methodology, writing (original draft), project administration. MJ: conceptualisation, funding acquisition, validation, investigation, methodology, writing (review and editing). TG, ME, ACC: resources, formal analysis, investigation, writing (review and editing). CO: conceptualisation, funding acquisition, validation, investigation, methodology, supervision, writing (review and editing). TLJ: resources,

conceptualisation, funding acquisition, validation, investigation, methodology, supervision, writing (review and editing).

References

1. Dehlin, M., L. Jacobsson, and E. Roddy, Global epidemiology of gout: prevalence, incidence, treatment patterns and risk factors. Nat Rev Rheumatol, 2020. 16(7): p. 380-390.
2. Abhishek, A., S.K. Tedeschi, T. Pascart, A. Latourte, N. Dalbeth, T. Neogi, et al., The 2023 ACR/EULAR Classification Criteria for Calcium Pyrophosphate Deposition Disease. Arthritis Rheumatol, 2023. 75: 1703-1713.
3. Neogi, T., T.L.T.A. Jansen, N. Dalbeth, J. Fransen, H.R. Schumacher, D. Berendsen, et al., 2015 Gout Classification Criteria: An American College of Rheumatology/European League Against Rheumatism Collaborative Initiative. Arthritis & Rheumatology, 2015. 67(10): p. 2557-2568.
4. Berendsen, D., T. Neogi, W.J. Taylor, N. Dalbeth, and T.L. Jansen, Crystal identification of synovial fluid aspiration by polarized light microscopy. An online test suggesting that our traditional rheumatologic competence needs renewed attention and training. Clin Rheumatol, 2017. 36(3): p. 641-647.
5. McGill, N.W. and H.F. York, Reproducibility of synovial fluid examination for crystals. Aust N Z J Med, 1991. 21(5): p. 710-3.
6. Schumacher, H.R., Jr., M.S. Sieck, S. Rothfuss, G.M. Clayburne, D.F. Baumgarten, B.S. Mochan, et al., Reproducibility of synovial fluid analyses. A study among four laboratories. Arthritis Rheum, 1986. 29(6): p. 770-4.
7. Bernal, J.A., M. Andrés, S. López-Salguero, V. Jovaní, P. Vela-Casasempere, and E. Pascual, Agreement Among Multiple Observers on Crystal Identification by Synovial Fluid Microscopy. Arthritis Care Res (Hoboken), 2022. 75: 682-688
8. Jost, A. and J. Waters, Designing a rigorous microscopy experiment: Validating methods and avoiding bias. The Journal of Cell Biology, 2019. 218: p. jcb.201812109.
9. McGill, N., P.A. Dieppe, M. Bowden, D.J. Gardiner, and M. Hall, Identification of pathological mineral deposits by Raman microscopy. Lancet, 1991. 337(8733): p. 77-8.
10. Abhishek, A., D.J. Curran, F. Bilwani, A.C. Jones, M.R. Towler, and M. Doherty, In vivo detection of monosodium urate crystal deposits by Raman spectroscopy—a pilot study. Rheumatology, 2015. 55(2): p. 379-380.
11. Li, B., N. Singer, Y. Yeni, D. Haggins, E. Barnboym, D. Oravec, et al., A point of care Raman spectroscopy based device to diagnose gout and pseudogout: Comparison with the clinical standard microscopic analysis. Arthritis & rheumatology (Hoboken, N.J.), 2016. 68.
12. Zhang, B., H. Xu, J. Chen, X. Zhu, Y. Xue, Y. Yang, et al., Highly specific and label-free histological identification of microcrystals in fresh human gout tissues with stimulated Raman scattering. Theranostics, 2021. 11(7): p. 3074-3088.
13. Niessink, T., C. Kuipers, B.Z. de Jong, A.T.M. Lenferink, M. Janssen, T.L. Jansen, et al., Raman hyperspectral imaging detects novel and combinations of crystals in synovial fluids of patients with a swollen joint. Journal of Raman Spectroscopy, 2023. 54(1): p. 47-53.

14. Li, H., Y. Zhou, Y. Wu, Y. Jiang, H. Bao, A. Peng, et al., Real-time and accurate calibration detection of gout stones based on terahertz and Raman spectroscopy. Frontiers in bioengineering and biotechnology, 2023. 11: p. 1218927.
15. Niessink, T., C. Otto, M. Janssen, and T.L. Jansen, Calcium carbonates are novel positive birefringent crystals in synovial fluid. Clinical Rheumatology, 2023. 42(2): p. 635-636.
16. Niessink, T., J. Ringoot, C. Otto, M. Janssen, and T.L. Jansen, Clinical Images: Detection of titanium dioxide particles by Raman spectroscopy in synovial fluid from a swollen ankle. Arthritis Rheumatol, 2022. 74(6): p. 1069.
17. Rosenthal, A.K., Basic calcium phosphate crystal-associated musculoskeletal syndromes: an update. Curr Opin Rheumatol, 2018. 30(2): p. 168-172.
18. Lorenz, E.C., C.J. Michet, D.S. Milliner, and J.C. Lieske, Update on oxalate crystal disease. Curr Rheumatol Rep, 2013. 15(7): p. 340.
19. Jansen, T.L., Lipid Crystals, in Synovial Fluid Analysis and The Evaluation of Patients With Arthritis, B.F. Mandell, Editor. 2022, Springer International Publishing: Cham. p. 115-124.
20. Niessink, T., T. Giesen, M. Efdé, A. Comarniceanu, M. Janssen, C. Otto, et al., Test characteristics of Raman spectroscopy integrated with polarized light microscopy for the diagnosis of acute gouty arthritis. Joint Bone Spine, 2023. 90(6): p. 105611.
21. Hajian-Tilaki, K., Sample size estimation in diagnostic test studies of biomedical informatics. J Biomed Inform, 2014. 48: p. 193-204.
22. Cohen, J.F., D.A. Korevaar, D.G. Altman, D.E. Bruns, C.A. Gatsonis, L. Hooft, et al., STARD 2015 guidelines for reporting diagnostic accuracy studies: explanation and elaboration. BMJ Open, 2016. 6(11): p. e012799.
23. McHugh, M.L., Interrater reliability: the kappa statistic. Biochem Med (Zagreb), 2012. 22(3): p. 276-82.
24. Darvin, M.E., J. Lademann, J. von Hagen, S.B. Lohan, H. Kolmar, M.C. Meinke, et al., Carotenoids in Human SkinIn Vivo: Antioxidant and Photo-Protectant Role against External and Internal Stressors. Antioxidants (Basel), 2022. 11(8).
25. Sapkal R.T, S.S. Shinde., K.Y. Rajpure, and C.H. Bhosale, Photoelectrocatrocatalytic hydrolysis of starch by using sprayed ZnO thin films. Journal of Semiconductors, 2013. 34(5): p. 053001.
26. Pascual, E. and V. Jovaní, Synovial fluid analysis. Best Practice & Research Clinical Rheumatology, 2005. 19(3): p. 371-386.
27. Oliviero, F. and B.F. Mandell, Synovial fluid analysis: Relevance for daily clinical practice. Best Practice & Research Clinical Rheumatology, 2023: p. 101848.
28. Jansen, T.L. and A. Spoorenberg, Medical Mystery: Arthritis — The Answer. New England Journal of Medicine, 2006. 355(4): p. 421-422.
29. Oliviero, F., P. Galozzi, R. Ramonda, F.L. de Oliveira, F. Schiavon, A. Scanu, et al., Unusual findings in synovial fluid analysis: A review. Annals of Clinical and Laboratory Science, 2017. 47(3): p. 253-259.
30. Li, B., N. Singer, A. Rosenthal, M. Unal, D. Haggins, Y.N. Yeni, et al., Chemical characterization of Maltese-cross birefringent particles in synovial fluid samples collected from symptomatic joints. Joint Bone Spine, 2018. 85(4): p. 501-503.
31. Barker, S.A., C.F. Hawkins, and M. Hewins, Mucopolysaccharides in synovial fluid detection of chondroitin sulphate. Ann Rheum Dis, 1966. 25(3): p. 209-13.
32. Kamemoto, L., A. Misra, S. Sharma, M. Goodman, H. Luk, and T. Acosta, Near-Infrared Micro-Raman Spectroscopy for in Vitro Detection of Cervical Cancer. Applied spectroscopy, 2010. 64: p. 255-61.

33. Ménard, H.A., R.D. Médicis, A. Brown, and J. Brown, Charcot-Leyden Crystals in Synovial Fluid. Arthritis & Rheumatism, 1981. 24(12): p. 1591-1593.
34. Rosenthal, A.K., Analytic Methods to Detect Articular Basic Calcium Phosphate Crystals, in Synovial Fluid Analysis and The Evaluation of Patients With Arthritis, B.F. Mandell, Editor. 2022, Springer International Publishing: Cham. p. 125-132.
35. Leslie, H.A., M.J.M. van Velzen, S.H. Brandsma, A.D. Vethaak, J.J. Garcia-Vallejo, and M.H. Lamoree, Discovery and quantification of plastic particle pollution in human blood. Environment International, 2022. 163: p. 107199.
36. Li, Z., Y. Zheng, Z. Maimaiti, J. Fu, F. Yang, Z.-Y. Li, et al., Identification and analysis of microplastics in human lower limb joints. Journal of Hazardous Materials, 2023: p. 132640.
37. Niessink, T., T. Jansen, M. Janssen, T. Welting, and C. Otto, POS0102 Calcium containing crystals are highly prevalent in joint fluid of advanced osteoarthritis of the knee. Annals of the Rheumatic Diseases, 2023. 82(Suppl 1): p. 264-264.
38. Campillo-Gimenez, L., F. Renaudin, M. Jalabert, P. Gras, M. Gosset, C. Rey, et al., Inflammatory Potential of Four Different Phases of Calcium Pyrophosphate Relies on NF-κB Activation and MAPK Pathways. Frontiers in Immunology, 2018. 9(2248).

Tables:

	Total	CPPD according to 2023 ACR/EULAR classification criteria	Non-CPPD according to 2023 ACR/EULAR classification criteria
Patient count	400	50 (100%)	350 (87.50%)
Clinical diagnosis			
Gout*	139 (34.8%)		139 (39.7%)
CPPD**	50 (12.5%)	50 (100%)	
Osteoarthritis[X]	35 (8.8%)		35 (10.0%)
Rheumatoid arthritis	40 (10.0%)		40 (11.4%)
Bacterial infection	11 (2.7%)		11 (3.2%)
Undefined	125 (31.2%)		125 (35.7%)
Sex			
Male	257 (64.3%)	30 (60.0%)	227 (64.9%)
Female	143 (35.7%)	20 (40.0%)	123 (35.1%)
Age (years)			
Mean age (SD)	66.2 (± 15.2)	74.8 (±10.2)	65.0 (±15.4)
Analysed joint or bursa			
MTP1***	77 (19.3%)	0 (0%)	77 (22.0%)
Ankle	43 (10.7%)	0 (0%)	43 (12.3%)
Knee	179 (44.7%)	38 (76.0%)	141(40.3%)
Wrist	23 (5.8%)	6 (12.0%)	17 (4.8%)
Other[§]	78 (19.5%)	6 (12.0%)	72 (20.6%)
PLM identification of CPP			
Present	38 (9.5%)	38 (76.0)	0 (0%)
Uncertain	48 (12.0%)	12 (24.0%)	38 (10.9%)
Not present	314 (78.5%)	0 (0%)	312 (89.1%)
Radiographic presence of chondrocalcinosis			
None[T]	322 (80.5)	5 (10.0%)	317 (90.5%)
Index joint	54 (13.5%)	44 (88.0%)	10 (2.9%
Any other peripheral joint	78 (19.5%)	45 (90.0%)	33 (9.5%)
ACR/EULAR points *Total awarded per patient*			
-11 to 25	308 (77.0%)	5 (10.0%)	303 (86.6%)
26 to 40	30 (7.5%)	0 (0%)	30 (8.6%)
41 to 56	20 (5.0%)	3 (6.0%)	17 (4.8%)
>57	42 (10.5%)	42 (84.0%)	0 (0%)

Table 1: Baseline patient characteristics. *Data are in averages (standard deviation) or n (%). *According to 2015 ACR/EULAR Gout classification criteria (2). **According to 2023 ACR/EULAR CPPD classification criteria (3). ***first metatarsophalangeal joint. § Other joints include hand, elbow, hip, shoulder, and bursae. [T]Of 4 patients, no*

recent radiographic imaging was available. [X]These only include patients with a clinical diagnosis of OA who were negative for the 2023 ACR/EULAR CPPD classification criteria.

	Patient scored ≥57 points on 2023 ACR/EULAR CPPD Criteria			Patient scored <57 points on 2023 ACR/EULAR CPPD Criteria		
	PLM CPP Certain	PLM CPP Suspected	PLM CPP Negative	PLM CPP Certain	PLM CPP Suspected	PLM CPP Negative
iRPolM CPP Positive	30	5[T]	0	8	2[T]	1
iRPolM CPP Negative	2	5[T]	0	0	36[T]	311
	Scenario 1 *iRPolM against the 2023 ACR/EULAR CPPD criteria set (uncertain identification disregarded in calculation of score)±*			**Scenario 2** *iRPolM against the 2023 ACR/EULAR CPPD criteria set (uncertain identification considered negative)§*		
Sensitivity	86.0% (73.2 - 94.1)			90.7% (77.7 - 97.4)		
Specificity	99.1% (97.5 - 99.8)			98.0% (96.0 - 99.2)		
Positive LR*	100.3 (32.3 - 311.3)			42.3 (22.1 - 96.2)		
Negative LR	0.14 (0.07 - 0.28)			0.09 (0.04 - 0.24)		
Positive PV**	93.5% (82.2 - 97.8)			84.8% (72.7 - 92.1)		
Negative PV	98.0% (82.2 - 97.8)			98.8% (98.2 - 99.6)		
Accuracy	97.5% (95.4 - 98.7)			97.3% (95.1 - 98.6)		
Kappa	0.88 *strong agreement*			0.86 *strong agreement*		
	Scenario 3 *iRPolM against PLM (Certain and Uncertain considered positive)*			**Scenario 4** *iRPolM against PLM (Only Certain considered positive)*		
Sensitivity	51.2% (40.3 - 62.0)			95.00% (83.09–- 99.39)		
Specificity	99.7% (98.2 - 99.9)			97.78% (95.67–- 99.04)		
Positive LR*	159.6 (22.3 - 1141.2)			42.75 (21.47–- 85.14)		
Negative LR	0.49 (0.40 - 0.16)			0.05 (0.01–- 0.20)		
Positive PV**	97.8% (86.3 - 99.7)			82.61% (70.46–- 90.44)		
Negative PV	87.9% (85.4 - 90.0)			99.44% (97.85–- 99.85)		
Accuracy	89.0% (85.5 - 91.9)			97.50% (95.45–- 98.79)		
Kappa	0.61 *moderate agreement*			0.87 *strong agreement*		

Table 2: Results of iRPolM compared to polarized light microscopic analysis and 2023 ACR/EULAR CPPD classification criteria set for three different scenarios. *Between brackets () 95% confidence interval. Uncertain outcomes are disregarded in the calculation of diagnostic performance measures. ± Patients are considered positive when either CPP crystals are identified with PLM with certainty or >56 points*

*can be awarded according to the 2023 ACR/EULAR CPPD classification criteria set. § ± Patients are considered positive when either CPP crystals are identified with PLM with certainty or >56 points can be awarded according to the 2023 ACR/EULAR CPPD classification criteria set. All uncertain PLM identifications are considered negative for CPP. *Likelihood ratio. ** Predictive value. [T] Alternative crystal identifications of the uncertain cases as per iRPolM are shown in supplementary information 1.*

Figure legends:

Figure 1: Schematic flow of participants*. Points were awarded based on symptoms, course of disease and radiology (CR). Uncertainty for CPP with PLM implies an indefinite outcome which was suspicious for the presence of positive birefringent crystals, whereas PLM negative indicates a clear absence of positive birefringent rhomboidal / tubular structures.*

Figure 2: Overview of birefringent crystals in the analysis of synovial fluids. *All displayed data has been collected from patients within the presented cohorts. Polarized light microscopy images taken with a Zeiss Axiolab 5 polarized light microscope. Abbreviations: PE = polyethylene terephthalate, PS = Polystyrene, PP = Polypropylene, PE = polyethylene.*

Figure 3: Raman spectra of Maltese cross birefringent objects. *All displayed data has been collected from patients within the presented cohort. Polysaccharide-like Maltese cross birefringent objects were found in two patients, monosodium urate-like Maltese cross birefringent objects were found in two hyperuricemic patients, and lipid-like Maltese cross birefringent objects were found in one patient.*

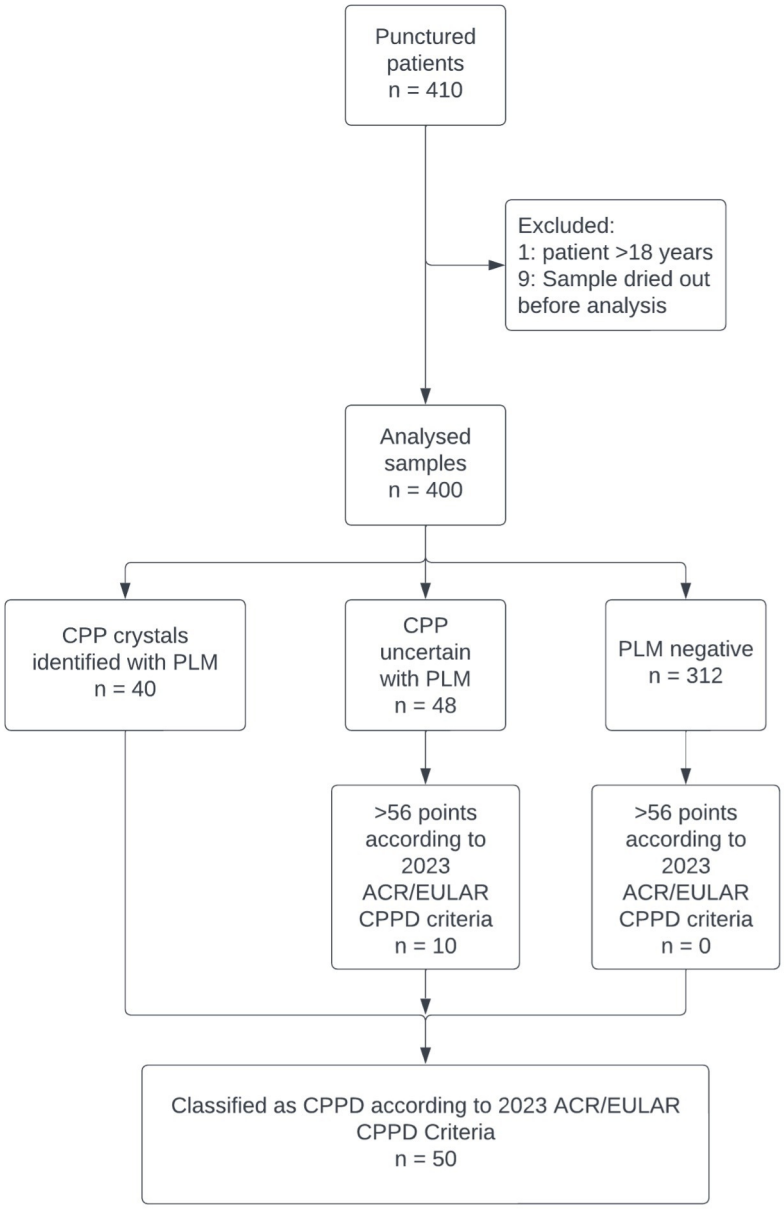

figure 1.jpg

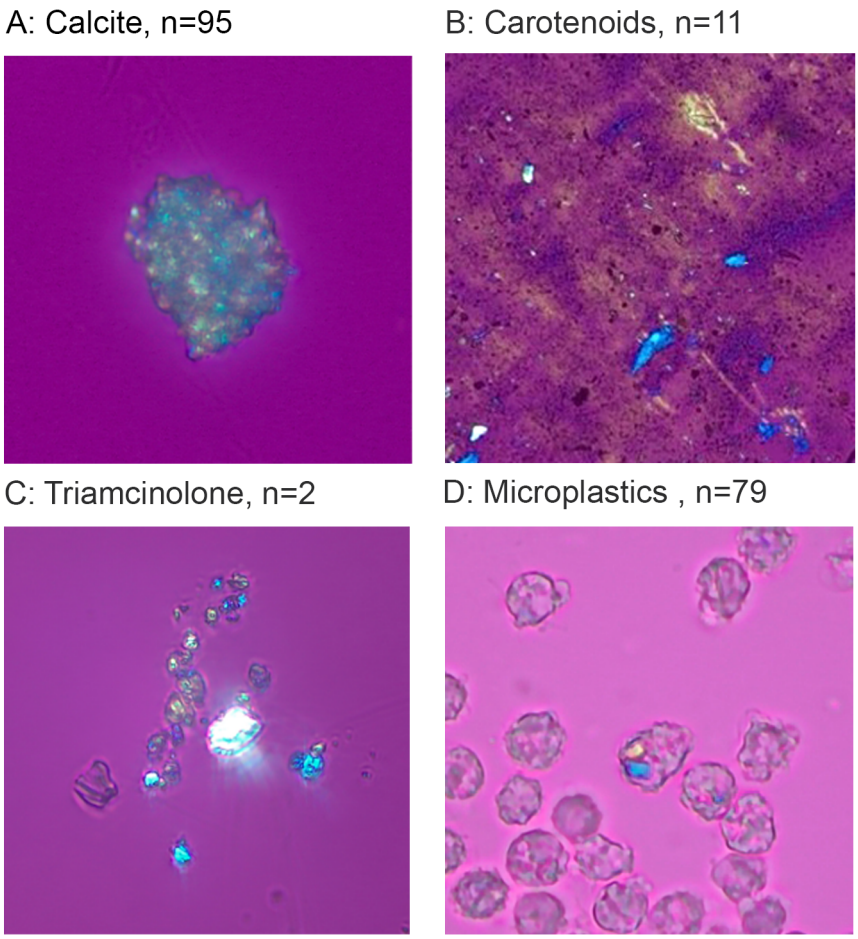

Figure 2.tif

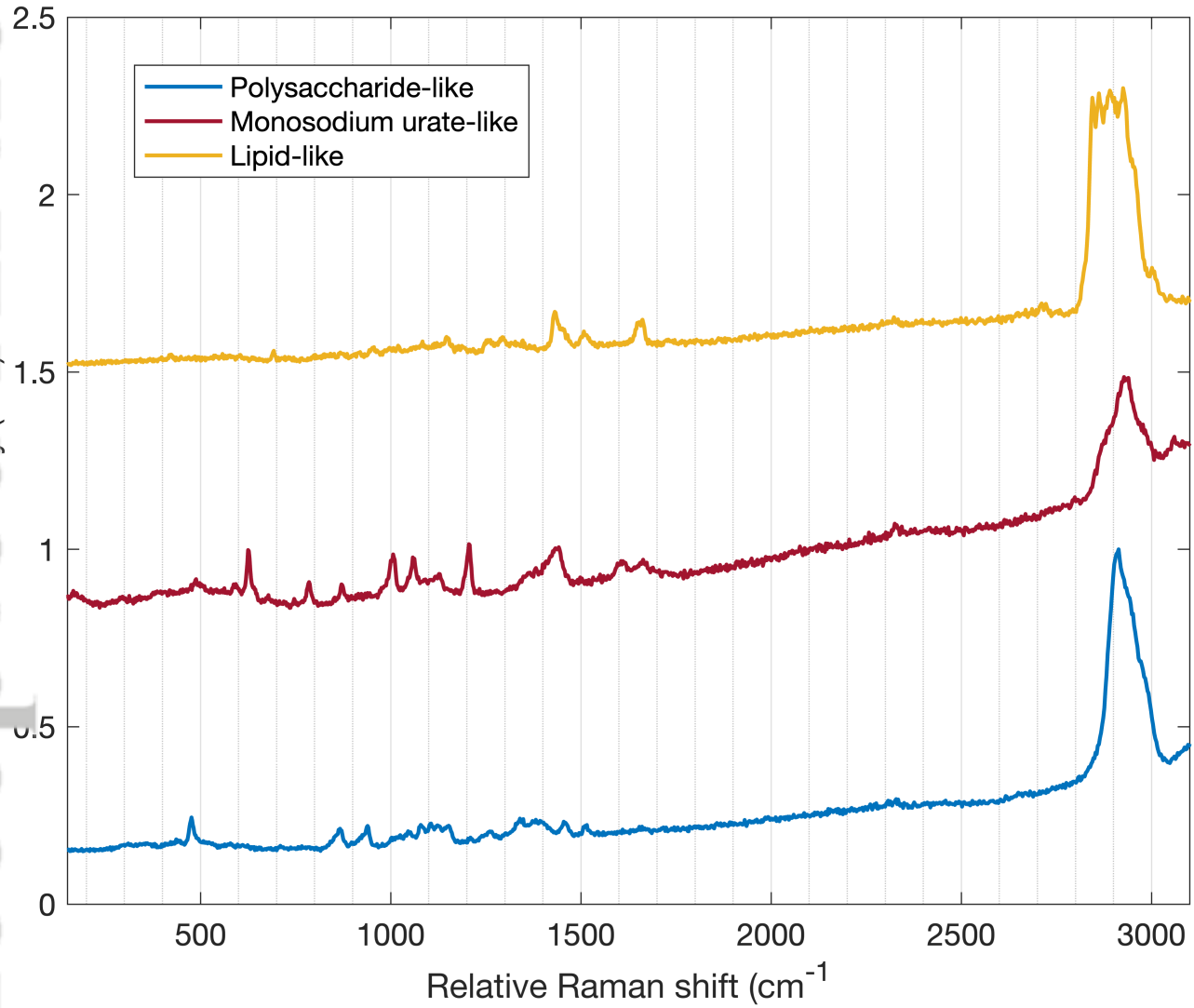

Figure 3.png